

Evidence for $B^- \rightarrow \tau^- \bar{\nu}_\tau$ with a Hadronic Tagging Method Using the Full Data Sample of Belle

K. Hara,¹¹ Y. Horii,³³ T. Iijima,^{33,32} I. Adachi,¹¹ H. Aihara,⁵² D. M. Asner,⁴² T. Aushev,¹⁸ T. Aziz,⁴⁸
 A. M. Bakich,⁴⁷ M. Barrett,¹⁰ V. Bhardwaj,³⁴ B. Bhuyan,¹³ A. Bondar,³ G. Bonvicini,⁵⁷ A. Bozek,³⁸
 M. Bračko,^{28,19} T. E. Browder,¹⁰ V. Chekelian,²⁹ A. Chen,³⁵ P. Chen,³⁷ B. G. Cheon,⁹ K. Chilikin,¹⁸ I.-S. Cho,⁵⁹
 K. Cho,²³ Y. Choi,⁴⁶ D. Cinabro,⁵⁷ J. Dalseno,^{29,49} J. Dingfelder,² Z. Doležal,⁴ Z. Drásal,⁴ A. Drutskoy,^{18,31}
 D. Dutta,¹³ S. Eidelman,³ D. Epifanov,³ S. Esen,⁵ H. Farhat,⁵⁷ A. Frey,⁸ V. Gaur,⁴⁸ N. Gabyshev,³ S. Ganguly,⁵⁷
 R. Gillard,⁵⁷ Y. M. Goh,⁹ B. Golob,^{60,19} J. Haba,¹¹ T. Hara,¹¹ K. Hayasaka,³³ H. Hayashii,³⁴ T. Higuchi,²²
 Y. Hoshi,⁵⁰ K. Inami,³² A. Ishikawa,⁵¹ R. Itoh,¹¹ Y. Iwasaki,¹¹ T. Iwashita,³⁴ T. Julius,³⁰ J. H. Kang,⁵⁹
 T. Kawasaki,⁴⁰ C. Kiesling,²⁹ H. O. Kim,²⁵ J. B. Kim,²⁴ J. H. Kim,²³ K. T. Kim,²⁴ M. J. Kim,²⁵ Y. J. Kim,²³
 K. Kinoshita,⁵ J. Klucar,¹⁹ B. R. Ko,²⁴ P. Kodyš,⁴ S. Korpar,^{28,19} R. T. Kouzes,⁴² P. Križan,^{60,19} P. Krokovny,³
 B. Kronenbitter,²¹ T. Kuhr,²¹ T. Kumita,⁵⁴ A. Kuzmin,³ Y.-J. Kwon,⁵⁹ J. S. Lange,⁶ S.-H. Lee,²⁴ J. Li,⁴⁵ Y. Li,⁵⁶
 J. Libby,¹⁴ C. Liu,⁴⁴ Y. Liu,⁵ Z. Q. Liu,¹⁵ D. Liventsev,¹⁸ D. Matvienko,³ K. Miyabayashi,³⁴ H. Miyata,⁴⁰
 R. Mizuk,^{18,31} G. B. Mohanty,⁴⁸ A. Moll,^{29,49} T. Mori,³² N. Muramatsu,⁴³ E. Nakano,⁴¹ M. Nakao,¹¹
 H. Nakazawa,³⁵ Z. Natkaniec,³⁸ M. Nayak,¹⁴ C. Ng,⁵² N. K. Nisar,⁴⁸ S. Nishida,¹¹ K. Nishimura,¹⁰ O. Nitoh,⁵⁵
 T. Nozaki,¹¹ T. Ohshima,³² S. Okuno,²⁰ S. L. Olsen,⁴⁵ C. Oswald,² H. Ozaki,¹¹ P. Pakhlov,^{18,31} G. Pakhlova,¹⁸
 C. W. Park,⁴⁶ H. K. Park,²⁵ T. K. Pedlar,²⁷ R. Pestotnik,¹⁹ M. Petrič,¹⁹ L. E. Pilonen,⁵⁶ M. Prim,²¹ M. Röhrken,²¹
 S. Ryu,⁴⁵ H. Sahoo,¹⁰ K. Sakai,¹¹ Y. Sakai,¹¹ S. Sandilya,⁴⁸ D. Santel,⁵ T. Sanuki,⁵¹ Y. Sato,⁵¹ O. Schneider,²⁶
 G. Schnell,^{1,12} C. Schwanda,¹⁶ A. J. Schwartz,⁵ K. Senyo,⁵⁸ O. Seon,³² M. E. Sevier,³⁰ M. Shapkin,¹⁷ C. P. Shen,³²
 T.-A. Shibata,⁵³ J.-G. Shiu,³⁷ B. Shwartz,³ A. Sibidanov,⁴⁷ F. Simon,^{29,49} P. Smerkol,¹⁹ Y.-S. Sohn,⁵⁹ A. Sokolov,¹⁷
 E. Solovieva,¹⁸ M. Starič,¹⁹ M. Sumihama,⁷ T. Sumiyoshi,⁵⁴ G. Tatishvili,⁴² Y. Teramoto,⁴¹ K. Trabelsi,¹¹
 T. Tsuboyama,¹¹ M. Uchida,⁵³ S. Uehara,¹¹ Y. Unno,⁹ S. Uno,¹¹ P. Urquijo,² Y. Ushiroda,¹¹ Y. Usov,³
 C. Van Hulse,¹ P. Vanhoefer,²⁹ G. Varner,¹⁰ K. E. Varvell,⁴⁷ V. Vorobyev,³ M. N. Wagner,⁶ C. H. Wang,³⁶
 M.-Z. Wang,³⁷ P. Wang,¹⁵ M. Watanabe,⁴⁰ Y. Watanabe,²⁰ K. M. Williams,⁵⁶ E. Won,²⁴ B. D. Yabsley,⁴⁷
 H. Yamamoto,⁵¹ Y. Yamashita,³⁹ Y. Yusa,⁴⁰ Z. P. Zhang,⁴⁴ V. Zhilich,³ V. Zhulanov,³ and A. Zupanc²¹

(Belle Collaboration)

¹University of the Basque Country UPV/EHU, 48080 Bilbao

²University of Bonn, 53115 Bonn

³Budker Institute of Nuclear Physics SB RAS and Novosibirsk State University, Novosibirsk 630090

⁴Faculty of Mathematics and Physics, Charles University, 121 16 Prague

⁵University of Cincinnati, Cincinnati, Ohio 45221

⁶Justus-Liebig-Universität Gießen, 35392 Gießen

⁷Gifu University, Gifu 501-1193

⁸II. Physikalisches Institut, Georg-August-Universität Göttingen, 37073 Göttingen

⁹Hanyang University, Seoul 133-791

¹⁰University of Hawaii, Honolulu, Hawaii 96822

¹¹High Energy Accelerator Research Organization (KEK), Tsukuba 305-0801

¹²Ikerbasque, 48011 Bilbao

¹³Indian Institute of Technology Guwahati, Assam 781039

¹⁴Indian Institute of Technology Madras, Chennai 600036

¹⁵Institute of High Energy Physics, Chinese Academy of Sciences, Beijing 100049

¹⁶Institute of High Energy Physics, Vienna 1050

¹⁷Institute of High Energy Physics, Protvino 142281

¹⁸Institute for Theoretical and Experimental Physics, Moscow 117218

¹⁹J. Stefan Institute, 1000 Ljubljana

²⁰Kanagawa University, Yokohama 221-8686

²¹Institut für Experimentelle Kernphysik, Karlsruher Institut für Technologie, 76131 Karlsruhe

²²*Kavli Institute for the Physics and Mathematics of the Universe, University of Tokyo, Kashiwa 277-8583*

²³*Korea Institute of Science and Technology Information, Daejeon 305-806*

²⁴*Korea University, Seoul 136-713*

²⁵*Kyungpook National University, Daegu 702-701*

²⁶*École Polytechnique Fédérale de Lausanne (EPFL), Lausanne 1015*

²⁷*Luther College, Decorah, Iowa 52101*

²⁸*University of Maribor, 2000 Maribor*

²⁹*Max-Planck-Institut für Physik, 80805 München*

³⁰*School of Physics, University of Melbourne, Victoria 3010*

³¹*Moscow Physical Engineering Institute, Moscow 115409*

³²*Graduate School of Science, Nagoya University, Nagoya 464-8602*

³³*Kobayashi-Maskawa Institute, Nagoya University, Nagoya 464-8602*

³⁴*Nara Women's University, Nara 630-8506*

³⁵*National Central University, Chung-li 32054*

³⁶*National United University, Miao Li 36003*

³⁷*Department of Physics, National Taiwan University, Taipei 10617*

³⁸*H. Niewodniczanski Institute of Nuclear Physics, Krakow 31-342*

³⁹*Nippon Dental University, Niigata 951-8580*

⁴⁰*Niigata University, Niigata 950-2181*

⁴¹*Osaka City University, Osaka 558-8585*

⁴²*Pacific Northwest National Laboratory, Richland, Washington 99352*

⁴³*Research Center for Electron Photon Science, Tohoku University, Sendai 980-8578*

⁴⁴*University of Science and Technology of China, Hefei 230026*

⁴⁵*Seoul National University, Seoul 151-742*

⁴⁶*Sungkyunkwan University, Suwon 440-746*

⁴⁷*School of Physics, University of Sydney, NSW 2006*

⁴⁸*Tata Institute of Fundamental Research, Mumbai 400005*

⁴⁹*Excellence Cluster Universe, Technische Universität München, 85748 Garching*

⁵⁰*Tohoku Gakuin University, Tagajo 985-8537*

⁵¹*Tohoku University, Sendai 980-8578*

⁵²*Department of Physics, University of Tokyo, Tokyo 113-0033*

⁵³*Tokyo Institute of Technology, Tokyo 152-8550*

⁵⁴*Tokyo Metropolitan University, Tokyo 192-0397*

⁵⁵*Tokyo University of Agriculture and Technology, Tokyo 184-8588*

⁵⁶*CNP, Virginia Polytechnic Institute and State University, Blacksburg, Virginia 24061*

⁵⁷*Wayne State University, Detroit, Michigan 48202*

⁵⁸*Yamagata University, Yamagata 990-8560*

⁵⁹*Yonsei University, Seoul 120-749*

⁶⁰*Faculty of Mathematics and Physics, University of Ljubljana, 1000 Ljubljana*

We measure the branching fraction of $B^- \rightarrow \tau^- \bar{\nu}_\tau$ using the full $\Upsilon(4S)$ data sample containing 772×10^6 $B\bar{B}$ pairs collected with the Belle detector at the KEKB asymmetric-energy e^+e^- collider. Events with $B\bar{B}$ pairs are tagged by reconstructing one of the B mesons decaying into hadronic final states, and $B^- \rightarrow \tau^- \bar{\nu}_\tau$ candidates are detected in the recoil. We find evidence for $B^- \rightarrow \tau^- \bar{\nu}_\tau$ with a significance of 3.0 standard deviations including systematic errors and measure a branching fraction $\mathcal{B}(B^- \rightarrow \tau^- \bar{\nu}_\tau) = [0.72_{-0.25}^{+0.27}(\text{stat}) \pm 0.11(\text{syst})] \times 10^{-4}$.

PACS numbers: 13.20.He, 14.40.Nd

The purely leptonic decay $B^- \rightarrow \tau^- \bar{\nu}_\tau$ [1] is of high interest since it provides a unique opportunity to test the Standard Model (SM) and search for new physics beyond the SM. A recent estimate of the branching fraction based on a global fit to the Cabibbo-Kobayashi-Maskawa (CKM) matrix elements [2] is $(0.73_{-0.07}^{+0.12}) \times 10^{-4}$ [3]. In the absence of new physics, a measurement of $B^- \rightarrow \tau^- \bar{\nu}_\tau$ provides a direct experimental determination of the product of the B meson decay constant and the magnitude of the CKM matrix element $f_B |V_{ub}|$. Physics beyond the SM, however, could significantly suppress or enhance $\mathcal{B}(B^- \rightarrow \tau^- \bar{\nu}_\tau)$ via exchange of a new charged

particle such as a charged Higgs boson from supersymmetry or from two-Higgs doublet models [4, 5].

Experimentally, it is challenging to identify the $B^- \rightarrow \tau^- \bar{\nu}_\tau$ decay because it involves more than one neutrino in the final state and therefore cannot be kinematically constrained. At e^+e^- B factories, one can reconstruct one of the B mesons in the $e^+e^- \rightarrow \Upsilon(4S) \rightarrow B\bar{B}$ reaction, referred to hereafter as the tag side (B_{tag}), either in hadronic decays or in semileptonic decays. One then compares properties of the remaining particle(s), referred to as the signal side (B_{sig}), to those expected for signal and background. The method allows us to sup-

press strongly the combinatorial background from both $B\bar{B}$ and continuum $e^+e^- \rightarrow q\bar{q}$ ($q = u, d, s, c$) processes.

The first evidence of $B^- \rightarrow \tau^- \bar{\nu}_\tau$ was reported by the Belle collaboration with a significance of 3.5 standard deviations (σ) including systematic uncertainty and a measured branching fraction of $[1.79_{-0.49}^{+0.56}(\text{stat})_{-0.51}^{+0.46}(\text{syst})] \times 10^{-4}$ [6]. This measurement used hadronic tags and a data sample corresponding to 449×10^6 $B\bar{B}$ events. This was followed by measurements by Belle using the semileptonic tagging method [7], and also by the BaBar collaboration using both hadronic [8] and semileptonic [9] tagging methods. The four results are consistent. An average branching fraction is found to be $(1.67 \pm 0.30) \times 10^{-4}$ [10], which is nearly 3σ higher than the estimate based on a global fit. Therefore it is important to improve the precision of the measurement.

In this paper, we present a new measurement of $B^- \rightarrow \tau^- \bar{\nu}_\tau$ using a hadronic tagging method and the full data sample of the Belle experiment. The analysis described here has a number of significant improvements, including an increased data sample (a factor of 1.7), significantly improved hadronic tagging efficiency (a factor of 2.2), and improved signal efficiency due to less restrictive selection requirements (a factor of 1.8). The combined effect of these improvements and the accompanying change in the signal to background ratio due to the looser selection criteria results in a reduction of the expected error by a factor of two. The new analysis has also improved systematic uncertainties.

We use a 711 fb^{-1} data sample containing 772×10^6 $B\bar{B}$ pairs collected with the Belle detector [11] at the KEKB e^+e^- collider operating at the $\Upsilon(4S)$ resonance [12]. About 80% of the data sample has been reprocessed using improved track finding and photon reconstruction. We use a dedicated Monte Carlo (MC) simulation based on GEANT [13] to determine the signal selection efficiency and study the background. In order to reproduce the effect of beam background, data taken with random triggers for each run period are overlaid on simulated events. The $B^- \rightarrow \tau^- \bar{\nu}_\tau$ signal MC events are generated by the EVTGEN package [14], with the radiative effects based on the PHOTOS code [15]. To model the backgrounds from continuum processes, $b \rightarrow c$ processes, semileptonic $b \rightarrow u$ processes, and other rare $b \rightarrow u, d, s$ processes, we use large MC samples corresponding to 6, 10, 20, and 50 times the integrated luminosity of the data sample, respectively.

The B_{tag} candidates are reconstructed in 615 exclusive charged B meson decay channels using an improved full-reconstruction algorithm [16]. An output full-reconstruction-quality variable \mathcal{N}_{tag} ranges from zero for combinatorial background and continuum events to unity if an unambiguous B_{tag} is obtained from the hierarchical neural network. We also use the energy difference $\Delta E = E_{B_{\text{tag}}} - E_{\text{CM}}/2$ and the beam-energy-constrained mass $M_{\text{bc}} = \sqrt{(E_{\text{CM}}/2)^2/c^4 - |\vec{p}_{B_{\text{tag}}}|^2/c^2}$, where E_{CM}

is the e^+e^- center-of-mass (CM) energy, and $E_{B_{\text{tag}}}$ and $\vec{p}_{B_{\text{tag}}}$ are the energy and the momentum, respectively, of the B_{tag} candidate defined in the CM frame. Charged B_{tag} candidates with $\mathcal{N}_{\text{tag}} > 0.03$, $-0.08 \text{ GeV} < \Delta E < 0.06 \text{ GeV}$, and $5.27 \text{ GeV}/c^2 < M_{\text{bc}} < 5.29 \text{ GeV}/c^2$ are selected. The tag efficiency (0.24%) and the purity (65%) are improved by factors of 1.7 and 1.2, respectively, compared to Ref. [6]. The number of B_{tag} 's obtained for the full data set is 1.8×10^6 . In the case of $B^- \rightarrow \tau^- \bar{\nu}_\tau$ signal, in which the $B\bar{B}$ event has lower than average particle multiplicity, the tag efficiency is 0.31%. This tag efficiency is 2.2 times higher than that in the previous analysis [6].

In events where B_{tag} candidates are reconstructed, we search for $B^- \rightarrow \tau^- \bar{\nu}_\tau$ decays. The τ^- lepton is identified in the $e^- \bar{\nu}_e \nu_\tau$, $\mu^- \bar{\nu}_\mu \nu_\tau$, $\pi^- \nu_\tau$, and $\pi^- \pi^0 \nu_\tau$ decay channels. Candidate events are required to have one track with charge opposite that of the B_{tag} candidate. The charged tracks are required to satisfy $dz < 3 \text{ cm}$ and $dr < 0.5 \text{ cm}$, where dz and dr are unsigned impact parameters relative to the interaction point along and perpendicular to the beam axis, respectively. Charged tracks are classified as electron, muon, and pion candidates after rejecting kaon and proton candidates [11]. Candidate $\tau^- \rightarrow \pi^- \pi^0 \nu_\tau$ events are required to have one π^0 candidate reconstructed from $\pi^0 \rightarrow \gamma\gamma$ in which neither daughter photon was used in the B_{tag} reconstruction. The invariant mass of the $\pi^- \pi^0$ state is required to be within 0.15 GeV of the nominal ρ^- mass [17]. Multiple neutrinos in the final state are distinguished using the missing mass squared variable $M_{\text{miss}}^2 = (E_{\text{CM}} - E_{B_{\text{tag}}} - E_{B_{\text{sig}}})^2/c^4 - |\vec{p}_{B_{\text{tag}}} + \vec{p}_{B_{\text{sig}}}|^2/c^2$, where $E_{B_{\text{sig}}}$ and $\vec{p}_{B_{\text{sig}}}$ are the energy and the momentum, respectively, of the B_{sig} candidate in the CM frame. To avoid potential backgrounds from $e^- \bar{\nu}_e$, $\mu^- \bar{\nu}_\mu$, $\pi^- K_L^0$, and $\rho^- K_L^0$, we require $M_{\text{miss}}^2 > 0.7 \text{ GeV}^2/c^4$.

After removing the particles from the B_{tag} candidate and the charged tracks and π^0 's from the B_{sig} candidate, there should be no other detected particles. We require that there be no extra charged tracks with $dz < 75 \text{ cm}$ and $dr < 15 \text{ cm}$ nor extra π^0 candidates (" π^0 veto") nor K_L^0 candidates (" K_L^0 veto"). The K_L^0 veto is based on the hit patterns in the K_L^0 detection system [11] that are not associated with any charged tracks. We define the extra energy E_{ECL} [6], which is the sum of the energies of neutral clusters detected in the electromagnetic calorimeter that are not associated with either the B_{tag} or the π^0 candidate from the $\tau^- \rightarrow \pi^- \pi^0 \nu_\tau$ decay. The signal has either zero or a small value of E_{ECL} , while background events tend to have larger values due to the contributions from additional neutral clusters. The selection criteria for B_{tag} and extra charged tracks are optimized to maximize the sensitivity in a signal enhanced region $E_{\text{ECL}} < 0.2 \text{ GeV}$. We retain candidate events in the range $E_{\text{ECL}} < 1.2 \text{ GeV}$, where the correlation between E_{ECL} and M_{miss}^2 is small for each background

component.

The signal detection efficiency is estimated based on MC samples after applying a correction for the B_{tag} reconstruction efficiency. The correction factor is obtained by fitting the M_{bc} distribution for an E_{ECL} sideband sample defined by $0.4 \text{ GeV} < E_{\text{ECL}} < 1.2 \text{ GeV}$, for which the kinematics is expected to be similar to the signal. The resulting efficiencies are summarized in Table I. The validity of the efficiency estimation is checked by using a semileptonic decay sample in which B_{sig} is reconstructed in the decay chain $B^- \rightarrow D^{*0} \ell^- \bar{\nu}_\ell$ ($\ell = e$ or μ) followed by $D^{*0} \rightarrow D^0 \pi^0$ and $D^0 \rightarrow K^- \pi^+$.

The signal yield is extracted from a two-dimensional extended maximum likelihood fit to E_{ECL} and M_{miss}^2 . The likelihood is

$$\mathcal{L} = \frac{e^{-\sum_j n_j}}{N!} \prod_{i=1}^N \sum_j n_j f_j(E_i, M_i^2), \quad (1)$$

where j is an index for the signal and background contributions, n_j and f_j are the yield and the probability density function (PDF), respectively, of the j^{th} contribution, E_i and M_i^2 are the E_{ECL} and M_{miss}^2 values in the i^{th} event, respectively, and N is the total number of events in the data. The signal component in $\tau^- \rightarrow \pi^- \nu_\tau$ candidate events includes large cross-feed contributions from $\tau^- \rightarrow \ell^- \bar{\nu}_\ell \nu_\tau$ and $\tau^- \rightarrow \pi^- \pi^0 \nu_\tau$ decays. The dominant background contribution is from $b \rightarrow c$ decays. The small backgrounds from charmless B decays and continuum processes are also included in the fit. In the final sample, the fractions of the backgrounds from $b \rightarrow c$ decays, charmless B decays, and continuum processes are estimated from MC to be 89.8%, 9.7%, and 0.5% for leptonic τ^- decays and 75.1%, 6.5%, and 18.4% for hadronic τ^- decays. The PDFs are constructed by taking products of one-dimensional histograms in E_{ECL} and M_{miss}^2 obtained from MC for all contributions except for cross-feed from $\tau^- \rightarrow \pi^- \pi^0 \nu_\tau$ decays in $\tau^- \rightarrow \pi^- \nu_\tau$ candidate events; for this component a two-dimensional histogram PDF is used to take into account the correlation originating from the misreconstructed π^0 .

The B decays in which only one charged particle is detected can make a peak near zero E_{ECL} and mimic the signal. These are predominantly $B^- \rightarrow D^{(*)0} \ell^- \bar{\nu}_\ell$ and $\bar{B}^0 \rightarrow D^{(*)+} \ell^- \bar{\nu}_\ell$ decays, where the D decays semileptonically or to a final state with one or more K_L^0 's. Charmless B decays such as $B^- \rightarrow \pi^0 \ell^- \bar{\nu}_\ell$, $K^- \nu \bar{\nu}$, $K_L^0 \pi^-$, $K^{*-} \gamma$, and $\mu^- \bar{\nu}_\mu \gamma$ can also contribute. The fraction in the signal enhanced region $E_{\text{ECL}} < 0.2 \text{ GeV}$ of these peaking decay modes over the total background is 32% according to the MC simulation.

The simulated E_{ECL} and M_{miss}^2 distributions in MC are validated using various control samples. A non-zero E_{ECL} value for the $B^- \rightarrow \tau^- \bar{\nu}_\tau$ signal component is due to beam background and split-off showers originating

from B_{tag} and B_{sig} decay products. The average contributions from these sources are 0.04 GeV, 0.12 GeV, and 0.08 GeV, respectively, per event in the signal MC sample. The simulated E_{ECL} distribution is checked with the $B^- \rightarrow D^{*0} \ell^- \bar{\nu}_\ell$ sample, which has a final state similar to the $B^- \rightarrow \tau^- \bar{\nu}_\tau$ signal if the D^{*0} decay products are removed. We also check the difference between the detector resolution in data and MC for M_{miss}^2 with the $B^- \rightarrow D^{*0} \ell^- \bar{\nu}_\ell$ sample. We confirm that the E_{ECL} distributions and M_{miss}^2 resolutions of data and MC are consistent for the $B^- \rightarrow D^{*0} \ell^- \bar{\nu}_\ell$ sample as shown in Figure 1. The background E_{ECL} and M_{miss}^2 descriptions by MC are checked using sidebands in M_{bc} and E_{ECL} , events with the B_{tag} reconstructed in a B^0 mode, and events with the same B_{sig} charge as the B_{tag} . The K_L^0 detection efficiency is calibrated using a $D^0 \rightarrow \phi K_S^0$ data sample by comparing the yields of $\phi \rightarrow K_L^0 K_S^0$ and $\phi \rightarrow K^+ K^-$ decays. We confirm the MC expectations for the E_{ECL} and M_{miss}^2 shapes and verify that the normalization agrees with data after the calibrations of the B_{tag} and K_L^0 reconstruction efficiencies.

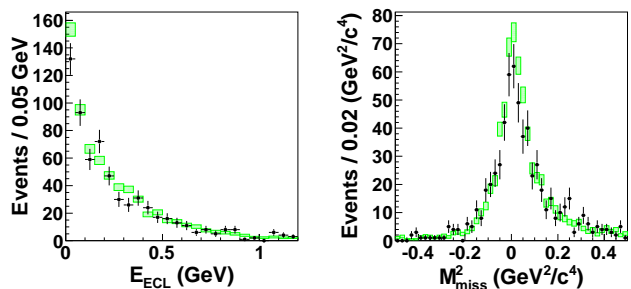


FIG. 1: Distributions of E_{ECL} (left) and M_{miss}^2 (right) for $B^- \rightarrow D^{*0} \ell^- \bar{\nu}_\ell$. The dots with error bars show the data. The rectangles show the normalized MC simulation, where the MC size is five times larger than the data.

In the final fit, five parameters are allowed to vary: the total signal yield and the sum of the backgrounds from $b \rightarrow c$ decays and continuum processes for each τ^- decay mode. The ratio of the $b \rightarrow c$ and continuum backgrounds is fixed to the value obtained from MC after the B_{tag} efficiency correction has been applied. The background contributions from charmless B decays are fixed to the MC expectation. We combine τ^- decay modes by constraining the ratios of the signal yields to the ratios of the reconstruction efficiencies obtained from MC including the branching fractions of τ^- decays [17].

Figure 2 shows the result of the fit to the E_{ECL} and M_{miss}^2 distributions for all the τ^- decay modes combined. The signal yield is $62_{-22}^{+23}(\text{stat}) \pm 6(\text{syst})$, where the first and second errors correspond to statistical and systematic uncertainties, respectively. The significance of the signal is estimated by $\sqrt{-2 \ln(\mathcal{L}_0/\mathcal{L}_{\text{max}})}$, where \mathcal{L}_{max} and \mathcal{L}_0 are the maximum likelihood and the likelihood

obtained assuming zero signal yield, respectively. The likelihoods are obtained after convolving with a Gaussian distribution that corresponds to the systematic error. We obtain a significance of 3.0σ including systematic uncertainties. The branching fraction is calculated by $\mathcal{B} = N_{\text{sig}}/(2\epsilon N_{B^+B^-})$, where N_{sig} is the signal yield, ϵ is the efficiency, and $N_{B^+B^-}$ is the number of B^+B^- events. Equal production of neutral and charged B meson pairs in $\Upsilon(4S)$ decay is assumed. We obtain

$$\mathcal{B}(B^- \rightarrow \tau^- \bar{\nu}_\tau) = [0.72_{-0.25}^{+0.27}(\text{stat}) \pm 0.11(\text{syst})] \times 10^{-4}. \quad (2)$$

The result is summarized in Table I.

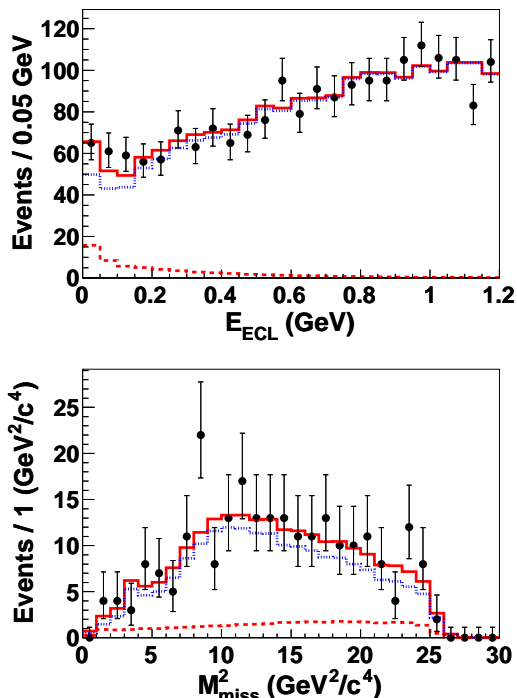


FIG. 2: Distributions of E_{ECL} (top) and M_{miss}^2 (bottom) combined for all the τ^- decays. The M_{miss}^2 distribution is shown for a signal region of $E_{\text{ECL}} < 0.2$ GeV. The solid circles with error bars are data. The solid histograms show the projections of the fits. The dashed and dotted histograms show the signal and background components, respectively.

As a check, we fit the E_{ECL} and M_{miss}^2 distributions while floating the yield for each of the four τ^- decay modes. The resulting yields, as well as the efficiencies and the branching fractions, are listed in Table I. We include the $e^- \bar{\nu}_e \nu_\tau$, $\mu^- \bar{\nu}_\mu \nu_\tau$, and $\pi^- \pi^0 \nu_\tau$ cross-feeds in the $\pi^- \nu_\tau$ candidate events in the $e^- \bar{\nu}_e \nu_\tau$, $\mu^- \bar{\nu}_\mu \nu_\tau$, and $\pi^- \pi^0 \nu_\tau$ signal yields. The branching fractions are in good agreement between different τ^- decays. We also check the result after removing the K_L^0 veto, and obtain $N_{\text{sig}} = 65_{-25}^{+27}(\text{stat})$ and $\mathcal{B}(B^- \rightarrow \tau^- \bar{\nu}_\tau) = [0.65_{-0.25}^{+0.27}(\text{stat})] \times 10^{-4}$. These checks are consistent with the nominal result. In addition, we perform one-dimensional fits to E_{ECL} and M_{miss}^2

and divide the data sample into several subsets. All results are in good agreement with the nominal result within the statistical errors.

TABLE I: Results of the fit for $B^- \rightarrow \tau^- \bar{\nu}_\tau$ yields (N_{sig}), detection efficiencies (ϵ), and branching fractions (\mathcal{B}). The efficiencies include the branching fractions of the τ^- decay modes. The errors for N_{sig} and \mathcal{B} are statistical only.

Sub-mode	N_{sig}	ϵ (10^{-4})	\mathcal{B} (10^{-4})
$\tau^- \rightarrow e^- \bar{\nu}_e \nu_\tau$	16_{-9}^{+11}	3.0	$0.68_{-0.41}^{+0.49}$
$\tau^- \rightarrow \mu^- \bar{\nu}_\mu \nu_\tau$	26_{-14}^{+15}	3.1	$1.06_{-0.58}^{+0.63}$
$\tau^- \rightarrow \pi^- \nu_\tau$	8_{-8}^{+10}	1.8	$0.57_{-0.59}^{+0.70}$
$\tau^- \rightarrow \pi^- \pi^0 \nu_\tau$	14_{-16}^{+19}	3.4	$0.52_{-0.62}^{+0.72}$
Combined	62_{-22}^{+23}	11.2	$0.72_{-0.25}^{+0.27}$

Systematic errors for the measured branching fraction are associated with the uncertainties in the signal yield, the efficiencies, and the number of B^+B^- pairs. The systematic error from MC statistics of the PDF histograms is evaluated by varying the content of each bin by its statistical uncertainty. To estimate the systematic error due to the possible signal E_{ECL} shape difference between MC and data, the ratio of data to MC for the E_{ECL} histograms of the $B^- \rightarrow D^{*0} \ell^- \bar{\nu}_\ell$ sample is fitted with a first-order polynomial and the signal E_{ECL} PDF is modified within the fitted errors. The uncertainties for the branching fractions of the B decays that peak near zero E_{ECL} are estimated by changing the branching fractions in MC by their experimental errors [17] if available, or by $\pm 50\%$ otherwise. The sizes of these backgrounds also depend on the fractions of the events with correctly reconstructed B_{tag} , and related systematic uncertainties are obtained by using the statistical errors for the fractions in the MC simulation. To estimate the uncertainty associated with the B_{tag} efficiency for the signal, $\mathcal{B}(B^- \rightarrow D^{*0} \ell^- \bar{\nu}_\ell)$ obtained from the $B^- \rightarrow D^{*0} \ell^- \bar{\nu}_\ell$ sample is compared to the world average value [17]. The results are consistent and the uncertainty of the measurement is assigned as the systematic error. The systematic errors in the signal-side efficiencies arise from the uncertainty in tracking efficiency, particle identification efficiency, π^0 reconstruction efficiency, branching fractions of τ^- decays, and MC statistics. The systematic uncertainty related to the K_L^0 veto efficiency is estimated from the statistical uncertainties of the $D^0 \rightarrow \phi K_S^0$ control sample and the fraction of events with K_L^0 candidates in the $B^- \rightarrow D^{*0} \ell^- \bar{\nu}_\ell$ sample. The total systematic error is calculated by summing the above uncertainties in quadrature. The estimated systematic errors are summarized in Table II.

The branching fraction measured here is lower than the previous Belle result with a hadronic tagging method [6]. Using the first sample of $449 \times 10^6 B\bar{B}$ pairs, which corresponds to the data set used in Ref. [6] after reprocessing,

TABLE II: Summary of the systematic errors for the $B^- \rightarrow \tau^- \bar{\nu}_\tau$ branching fraction measurement.

Source	\mathcal{B} syst. error (%)
Signal PDF	4.2
Background PDF	8.8
Peaking background	3.8
B_{tag} efficiency	7.1
Particle identification	1.0
π^0 efficiency	0.5
Tracking efficiency	0.3
τ branching fraction	0.6
MC efficiency statistics	0.4
K_L^0 efficiency	7.3
$N_{B^+B^-}$	1.3
Total	14.7

we obtain $\mathcal{B}(B^- \rightarrow \tau^- \bar{\nu}_\tau) = [1.08_{-0.35}^{+0.37}(\text{stat})] \times 10^{-4}$. Note that 89% of the events in the final sample in this analysis is not included in the final sample in Ref. [6] mainly due to the loosened selection, the different B_{tag} reconstruction method, and the K_L^0 veto. Using the last $323 \times 10^6 B\bar{B}$ pairs, we obtain $\mathcal{B}(B^- \rightarrow \tau^- \bar{\nu}_\tau) = [0.24_{-0.34}^{+0.39}(\text{stat})] \times 10^{-4}$, which is statistically consistent with the result for the first $449 \times 10^6 B\bar{B}$ data set within 1.6σ . Our results are also consistent with other publications within the errors [7–9].

In summary, we measure the branching fraction of the decay $B^- \rightarrow \tau^- \bar{\nu}_\tau$ with hadronic tagging using Belle’s final data sample containing $772 \times 10^6 B\bar{B}$ pairs. We find evidence for $B^- \rightarrow \tau^- \bar{\nu}_\tau$ with a signal significance of 3.0σ including systematic uncertainties and measure a branching fraction of $[0.72_{-0.25}^{+0.27}(\text{stat}) \pm 0.11(\text{syst})] \times 10^{-4}$. By employing a neural network-based method for hadronic tagging and a two-dimensional fit for signal extraction, along with a larger data sample, both statistical and systematic precisions are significantly improved compared to the previous analysis [6]. The result presented in this paper supersedes the previous result reported in Ref. [6]. Combined with the Belle measurement based on a semileptonic B tagging method [7] taking into account all the correlated systematic errors, the branching fraction is found to be $\mathcal{B}(B^- \rightarrow \tau^- \bar{\nu}_\tau) = (0.96 \pm 0.26) \times 10^{-4}$, with a 4.0σ signal significance including systematic uncertainties. This value is consistent with the SM expectation obtained from other experimental constraints. Using this result and parameters found in Ref. [17], we obtain

$f_B |V_{ub}| = [7.4 \pm 0.8(\text{stat}) \pm 0.5(\text{syst})] \times 10^{-4}$ GeV. Our result provides stringent constraints on various models of new physics including charged Higgs bosons.

We thank the KEKB group for excellent operation of the accelerator; the KEK cryogenics group for efficient solenoid operations; and the KEK computer group, the NII, and PNNL/EMSL for valuable computing and SINET4 network support. We acknowledge support from MEXT, JSPS and Nagoya’s TLPRC (Japan); ARC and DIISR (Australia); NSFC (China); MSMT (Czechia); DST (India); INFN (Italy); MEST, NRF, GSDC of KISTI, and WCU (Korea); MNiSW (Poland); MES and RFAAE (Russia); ARRS (Slovenia); SNSF (Switzerland); NSC and MOE (Taiwan); and DOE and NSF (USA). We are grateful for the support of JSPS KAK-ENHI Grant Number 24740157.

-
- [1] Charge-conjugate decays are implied throughout this paper unless otherwise stated.
 - [2] M. Kobayashi and T. Maskawa, *Prog. Theor. Phys.* **49**, 652 (1973); N. Cabibbo, *Phys. Rev. Lett.* **10**, 531 (1963).
 - [3] J. Charles *et al.* (CKMfitter Group), *Eur. Phys. J. C* **41**, 1 (2005), and preliminary results as of winter 2012 at <http://ckmfitter.in2p3.fr>.
 - [4] W. S. Hou, *Phys. Rev. D* **48**, 2342 (1993).
 - [5] S. Baek and Y. G. Kim, *Phys. Rev. D* **60**, 077701 (1999).
 - [6] K. Ikado *et al.* (Belle Collaboration), *Phys. Rev. Lett.* **97**, 251802 (2006).
 - [7] K. Hara *et al.* (Belle Collaboration), *Phys. Rev. D* **82**, 071101(R) (2010).
 - [8] J. P. Lees *et al.* (BaBar Collaboration), arXiv:1207.0698.
 - [9] B. Aubert *et al.* (BaBar Collaboration), *Phys. Rev. D* **81**, 051101(R) (2010).
 - [10] Y. Amhis *et al.* (Heavy Flavor Averaging Group), arXiv:1207.1158.
 - [11] A. Abashian *et al.* (Belle Collaboration), *Nucl. Instrum. Methods Phys. Res., Sect. A* **479**, 117 (2002).
 - [12] S. Kurokawa and E. Kikutani, *Nucl. Instrum. Methods Phys. Res., Sect. A* **499**, 1 (2003), and other papers included in this volume.
 - [13] R. Brun *et al.*, GEANT3.21, CERN Report DD/EE/84-1 (1984).
 - [14] D. J. Lange, *Nucl. Instrum. Methods Phys. Res., Sect. A* **462**, 152 (2001).
 - [15] E. Barberio and Z. Waş, *Comput. Phys. Commun.* **79**, 291 (1994).
 - [16] M. Feindt *et al.*, *Nucl. Instrum. Methods Phys. Res., Sect. A* **654**, 432 (2011).
 - [17] J. Beringer *et al.* (Particle Data Group), *Phys. Rev. D* **86**, 010001 (2012).